

FORMATION OF A VIBROFLUIDIZED FINE-GRAIN BED

A. F. Ryzhkov and B. A. Putrik

UDC 532.546

Based on an analysis of the nonlinear equation of dynamics, the mechanism for granular mass expansion (dilatation) and the vibrating packed bed parameters are discussed and compared with experiment.

1. Description of the Phenomenon. After vibration has been applied, the granular bed undergoes some structural-rheological changes and becomes highly movable. This defines the consumption properties of a vibrofluidized bed (VB). The VB states typical of separate stages of the evolution process (Fig. 1) are intimately connected with the current dynamic situation and repeat the known [1] vibrofluidization modes systematized in Table 1.

At the initial stage, the loose random packed bed (ε_0) is ordered, and the bed gives rise to a state of new (dynamic) equilibrium (ε_0). In this situation, the medium retains its combined state and can transfer mechanical stresses in the process of mutual grain movements initiated by applying superlimiting inertia loads that promote a vibropacking of the mixture. This state stops the evolution of the coarse-particle bed* under low-intensity vibration $K_{vi} = 0.8-2$ (curve 1 in Fig. 1b). As K_{vi} increases, the mutual slip of coarse grain increases, the packed bed is replaced by a looser one, and the porosity approaches the critical value ε_{cr} at which shear deformation does not cause any more bed volume changes (curve 2 in Fig. 1b).

In a fine-particle medium, the microoscillations cause noticeable gas pressure pulsations to occur in pore spacings and the gas to flow from excess-pressure regions. In this case the porosity fluctuations lead to pulsations of the packed bed resistance coefficient $\beta(\varepsilon)$ and the gas flowrate, thus exciting the resultant liquid flow and changing the mean bed core pressure. The process is accompanied by changes in the packed bed volume and structure, internal friction forces, and stability of the VB.

2. Rheodynamic Vibrofluidization Model. Theoretically, the transient process is an example of the slow rheological properties under vibration. Such problems are encountered in processing heterogeneous media (vapor-liquid systems, composite materials [3, 4]). Because of their complexity, these problems are analyzed by ordinary numerical methods.

Using the principles of modeling of the dynamic processes in a vibrating granular bed [5, 6], we write the *dynamics equation* for a dispersed phase with variable coefficients as

$$\ddot{X} + \omega_\varepsilon^2 \tau_V \dot{X} + \omega_\varepsilon^2 X = -\ddot{X}_{vi} - g(1 + \alpha). \quad (1)$$

Coinciding in structure with the earlier derived equation [5, 6], Eq. (1) includes the coefficients $\omega_\varepsilon, \tau_V$ which are dependent on the current porosity $\varepsilon(t)$ of the granular bed.

As usual [7], let us present the bed-to-environment gas exchange by the Darcy law:

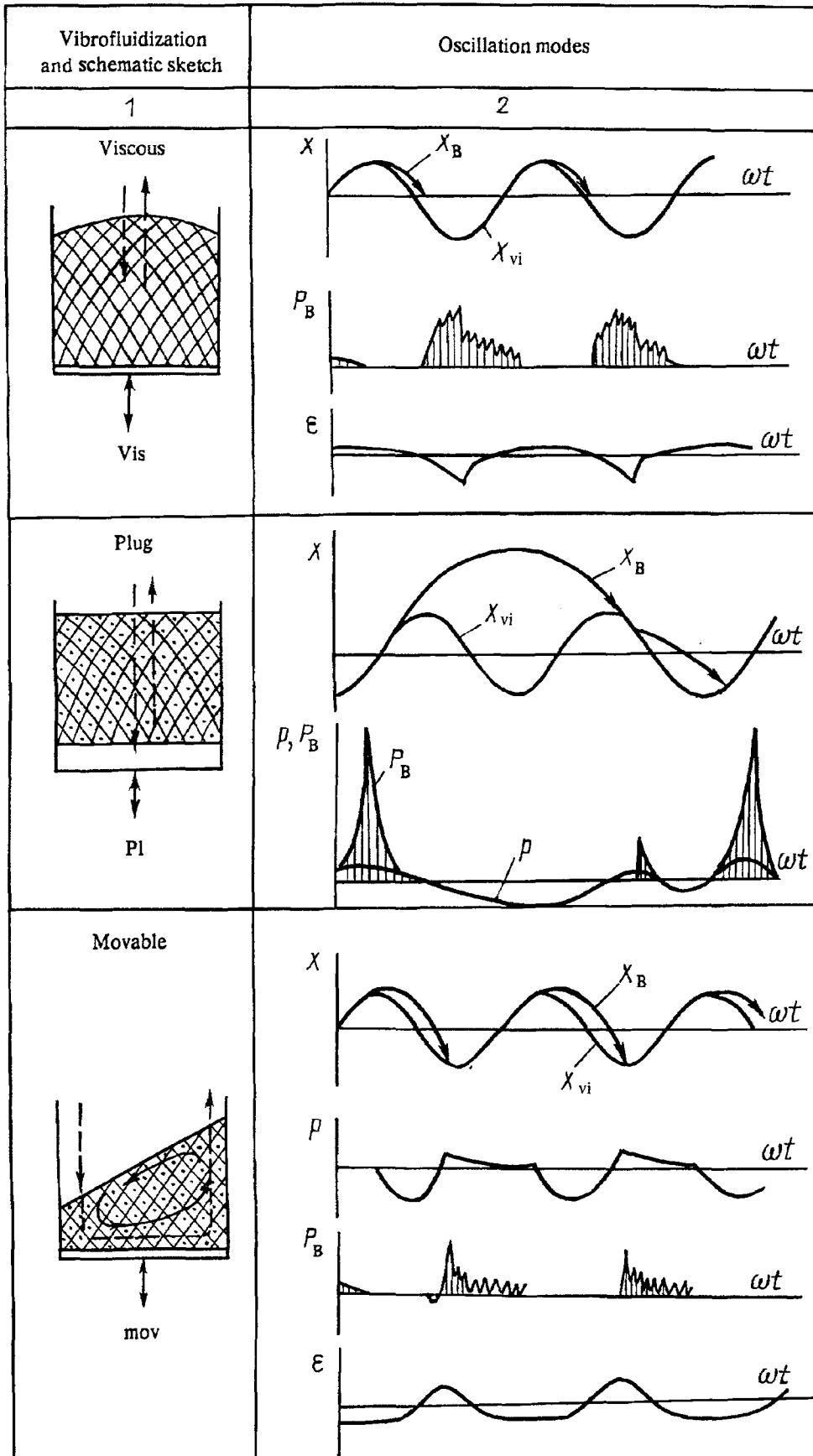
$$\dot{m} = -k_\varepsilon p / (P_0 + p). \quad (2)$$

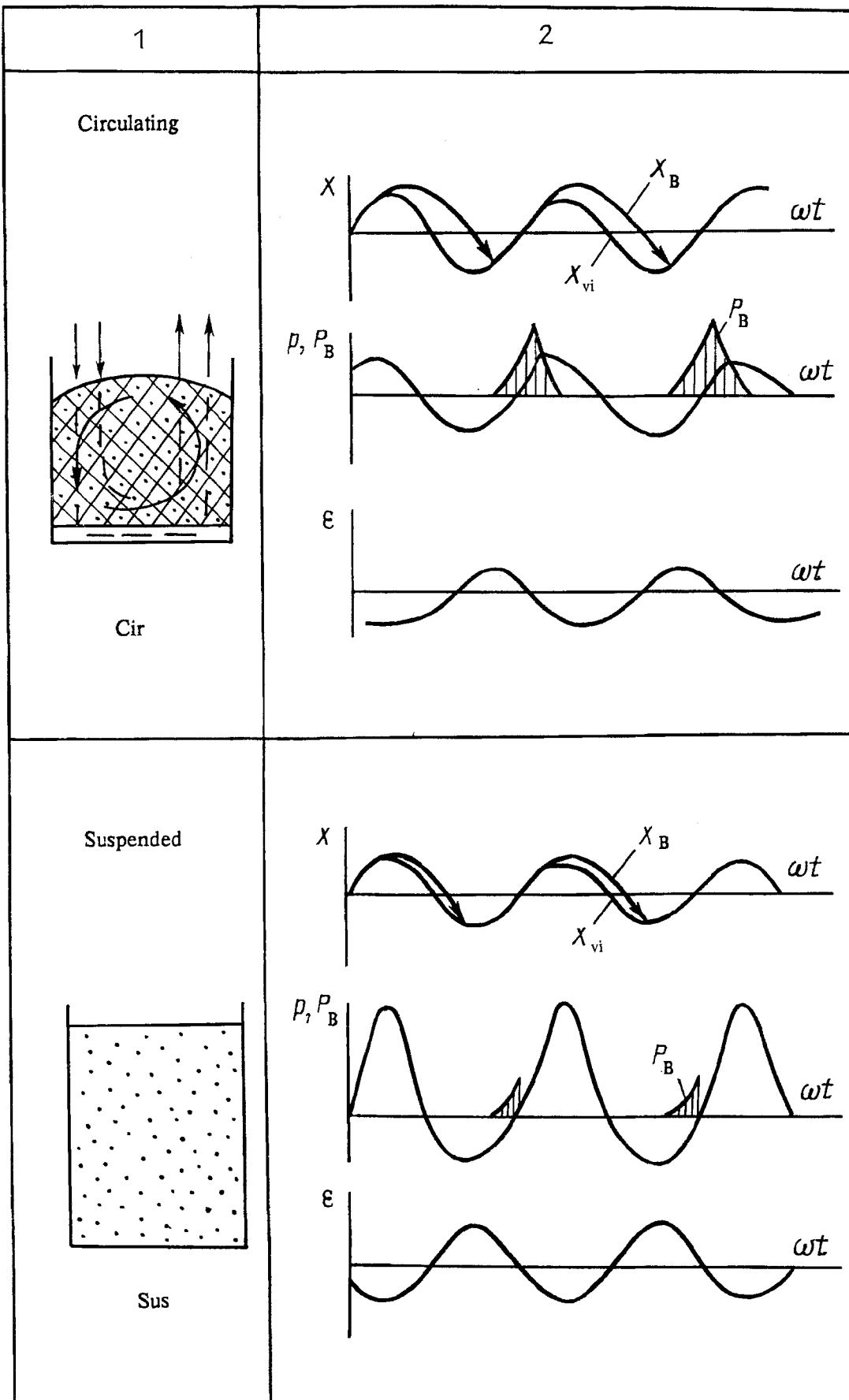
The nonzero specific flow \dot{m} through the free bed boundary causes the corresponding amount of gas in it to vary:

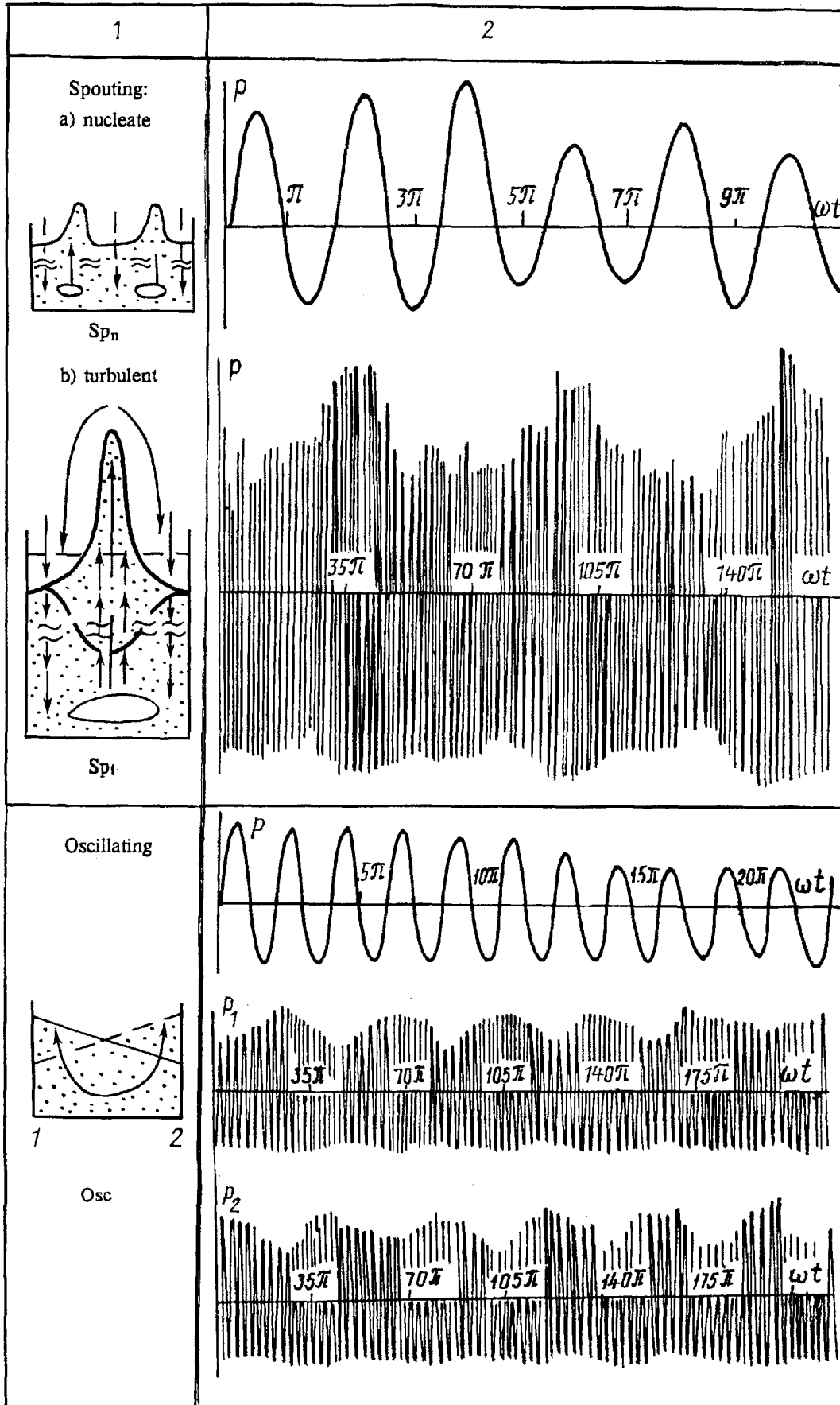
$$\dot{m} = \frac{d}{dt} (\rho \varepsilon H). \quad (3)$$

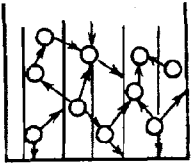
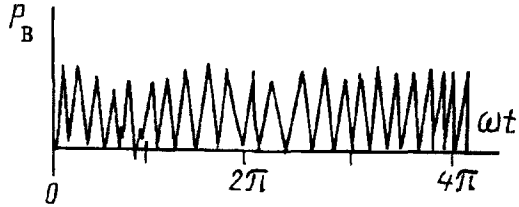
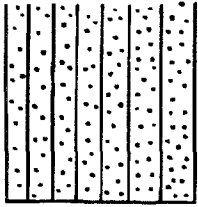
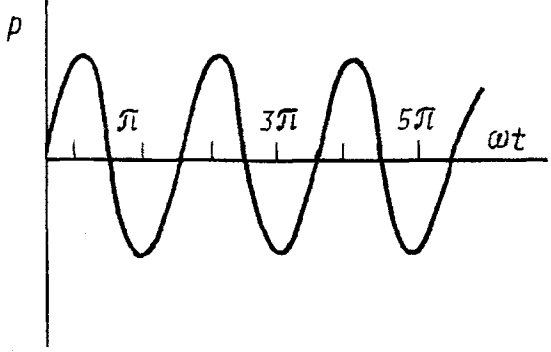
* Here the VB sizing classification cited elsewhere in [2] is used.

Catalogue of the Main Structures of a Vibrofluidized Bed




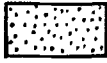


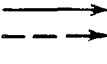
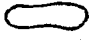
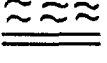






1	2
<p>Rarefied</p>  <p>Rr</p>	
<p>Pulsating gas suspension</p>  <p>G</p>	

Structure notations:

-  — internal packed
-  — dense
-  — transient from dense to expanded, loose or mixed
-  — expanded
-  — diluted
-  — pure gas
-  — particle and gas trajectories
-  — gas bubble
-  — discontinuity and flipping regions

Solving Eqs. (2) and (3) simultaneously, we obtain the *equation for bed expansion*:

$$\dot{\varepsilon} + \varepsilon(1 - \varepsilon) \frac{\dot{p}}{p_0 + p} - \frac{\dot{m}}{H} (1 - \varepsilon) = 0. \quad (4)$$

The presence of gas leaks, described by a relaxation term of Maxwell type (2), does not change the bed force structure. Therefore, the excess gas pressure p in the bed, as before [5], will be found in the form of a sum of the elastic and viscous components (*compression equation*):*

$$p = \rho_m(1 - \varepsilon) H_0 \omega_e^2 (X + \tau_v \dot{X}). \quad (5)$$

As the initial conditions we assume

$$t = 0: X = 0, \quad \dot{X} = V_{vi}, \quad \varepsilon = \varepsilon_0, \quad H = H_0. \quad (6)$$

The system (1)-(6) allows numerical studies of transient and steady conditions in the vibrobed to be made without using the empirical data. This has been done by the fourth-order Runge-Kutta method. Calculations have been performed over the frequency range $\Theta_v = 1 \cdot 10^{-5} - 1.7$, providing a coincidence between the model and the object [6]. Many of the obtained results have been compared with the known experimental data.

3. Vibrofluidization Dynamics in the Transient Process. Expansion. Vibration imposed on model systems composed of particles less than 100-150 μm causes them to expand (Figs. 2, 3) at a vibrovelocity above the critical velocity V_{cr} . Systems of coarser particles at ordinary vibration frequencies (10-100 Hz) and velocities (0.1-1 m/sec) do not expand.

The vibrofluidization curves for expansion of finely disperse systems are saturating by nature (Fig. 2b). The ultimate expansion attains its largest magnitude at low frequencies (LF) (10 and 20 Hz). Here the dependence of the system expansion on the vibrovelocity has the form of a characteristic crisis jump, which is seen in some studies [8].

Further expansion of the model system proceeds until the limiting frequency $\Theta_{cr} = 1.7$ is attained, at which the character of the forces of interphase interaction changes and the hydrodynamic resistance of the bed [6] decreases. In this case, the expansion of the system proceeds beyond the stability of a real granular bed ($\varepsilon_{vi} > \varepsilon_{max}$). This explains the development of nonuniform vibrofluidization regimes [1] and the excess of the design porosity over the real one (Fig. 2a).

At higher frequencies (HF) (40 and 50 Hz) the expansion of the model system changes smoothly with increasing vibration velocity, and the limiting frequency Θ_{cr} is attained in the region of stable granular bed structures ($\varepsilon_{vi} < \varepsilon_{max}$). Therefore, it is not surprising that the real system vibrates here always in the uniform state [9].

For vibrations with a frequency of 100 Hz and above the limiting value is achieved at a vibrovelocity not greater than the critical one V_{cr} . This suggests a transition to vibrating packed bed regimes (see the footnote), which is of great significance in practice [10].

Elevating the finely disperse packed bed temperature shifts the bed dilatation effect into the region of coarser particles since the free path traversed by molecules increases and the gas viscosity increases.

Thus, heating a bed of particles $\approx 70 \mu\text{m}$ in size to $\approx 1200 \text{ K}$ (μ increases approximately twice) leads to approximately the same expansion as the doubling of the vibration velocity under normal conditions. If we recall that, with increasing temperature, the combined state of the dispersed mass usually first decreases (due to the disappearance of capillary and adsorption moisture, electrostatic charge, etc.), then (due to grain melting and

* Neglecting the dry friction forces for initially loose ($\varepsilon_0 \approx \varepsilon_{cr}$) beds exerts no influence on the qualitative aspect of the phenomenon, reducing only the computational time of the transient process by 30-50%. This is of no practical importance. If negative dilatation effects ($\varepsilon_{vi} < \varepsilon_0$) are attained in the calculations, these should be considered as evidence of the development of the vibrating packed bed regime with strong particle interaction under bed compression.

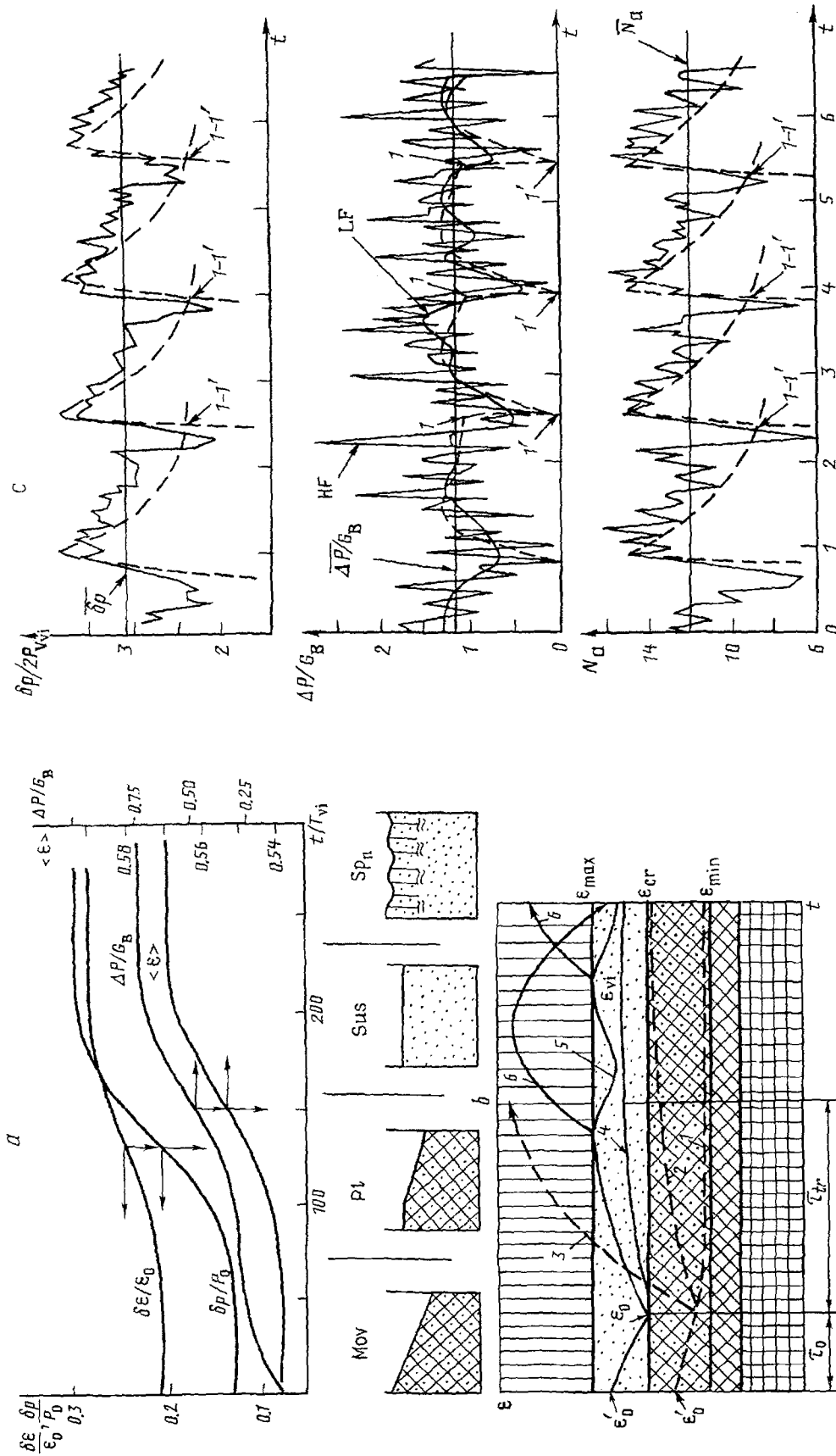


Fig. 1. Phenomenology of the vibrobed formation: a) evolution of the parameters and states of the corundum particle-containing VB, $d = 70 \mu\text{m}$, $V_{vl} = 0.235 \text{ m/sec}$, $f = 15 \text{ Hz}$, the height is resonant according to [11]; b) idealized dilatation VB curves in the transient process: 1) packed bed (Vis); 2) loosened bed (Rr); 3) rarefied bed (Rr); 4) uniform (Sus) and 5) nonuniform (Spn, SpI) expansion; 6) gas suspension (G); τ_0 , τ_{tr} initial and transient periods (structure notations are according to Table); c) time variation of the pulsation amplitudes of a gas pressure, mean gas pressure beneath the bed and power consumptions for corundum $70 \mu\text{m}$ diameter particle vibrofluidization within the spouting regime ($V_{vl} = 0.75 \text{ m/sec}$, $f = 20 \text{ Hz}$). The recording is synchronous [11]; dashed curves, calculation by (1)-(6); 1-1', process discontinuity lines (points) in the calculation. N_a , kW/m^2 ; t , sec.

softening) sharply increases, it is not difficult to select the optimal vibroprocessing temperature of the dispersed material.

A weaker (~twice) dilatation effect is attained by reducing the initial pressure P_0 (by increasing the kinematic gas viscosity and the Knudsen number).

Increasing the particle density reduces the expansion of the system since it is accompanied by the dimensionless frequency Θ_v approaching the upper limit Θ_{cr} .

The expansion of the finely disperse system is nonmonotonic. The considerable change in the natural frequency of oscillations during expansion gives rise to classical beats with frequency $\omega_{LF} \simeq |\omega - \omega_\varepsilon|$ intrinsic to sharp-resonant oscillatory systems with a high Q-factor of the circuit. These beats mainly define the physical aspect of LF fluctuations of the volume of the finely disperse VBs within the spouting regime.

The character of the dependence of the critical vibrovelocity on the particle diameter for all the investigated system parameters (ρ_m, P_0, T, ω) is close to quadratic and is uniquely described by a time-dependent power function of the phase velocity relaxation τ_{v0} calculated through the initial bed expansion porosity ε_0 (Fig. 3d):

$$V_{cr} = 126\tau_{v0}^{0.7} \gtrsim gK_\varepsilon/\omega \equiv V_\alpha.$$

Decreasing the particle size reduces the critical vibrovelocity V_{cr} up to $\leq V_\alpha$ [5] which results from overcoming of the dry friction forces at rest by the elastic forces. In this case, no bed porosity pulsations will be excited. Thus, the expansion of the finely disperse VBs is expected to begin at $V_{vi} \simeq V_\alpha > V_{cr}$. This is supported by numerous data on the appearance of the critical vibration velocity (determined through the incipient sharp increase in the heat and mass transfer coefficients, etc.) as a function of frequency of vibrations, some of which are shown in Fig. 3d. The threshold value of the vibration acceleration enabling porosity fluctuations to arise and the possibility to expand the bed is $K_\varepsilon = 4/\pi\alpha$ according to [11]. During vibroprocessing of the initially dense beds ($\alpha = 1$) $K_\varepsilon = 1.273$. For preliminarily expanded beds (e.g., due to gas blowing) $\alpha = 0.124-0.169$ [5] and, according to calculations, $K_\varepsilon = 0.16-0.23$. In practice, these values of K_ε are 1.2-1.5 and 0.3, respectively.

Hydrodynamic Resistance. Under laboratory conditions the change from the stationary to the vibrofluidized state takes place in the form of an instantaneous ($\tau_{tr} \sim 10^0$ sec) jump, whose inertia effects become perceptible. This is well represented by the vibrorheological equation constructed by using the direct motion separation method [3]:

$$m_b \langle \ddot{X} \rangle = \Delta P - G_b,$$

where the mean bed pressure drop ΔP serves as the so-called "vibration" forces. It is expedient that the equation should be used for a qualitative analysis of the calculation results and observations [11]. In addition, it should be noted that for $V_{vi} > V_{cr}$ the quantity ΔP practically everywhere exceeds the material column weight, hence the bed expands at an accelerated pace. The bed resistance is greatest in the domain of the bend of the curve $\langle \varepsilon \rangle (t)$ where the inertia forces are maximum. As the dynamic equilibrium state is approached, the pressure curve $\Delta P(t)$ (after a characteristic peak) asymptotically approaches a value corresponding to the condition for stationary granular bed suspension

$$\Delta P = G_b.$$

The obtained results make it possible to explain the excess "mean pressures" compared to G_B and the rarefactions within different real vibrofluidization regimes [9, 12], including those under combined fluidization [13]. In fluidized bed (FB) theory, accounting for slow inertia processes permits a successful description of relaxation oscillations in a large-volume sublattice-equipped apparatus [14]; the hydraulic resistance of a pulsating bed [1, p. 48] provides an insight into the pressure peak in the fluidization curve*, etc.

* It should be noted that the nonuniqueness of this concept statement [15, p. 56] is more likely connected with the fact that there are no quantitative calculations than with nonphysical notions.

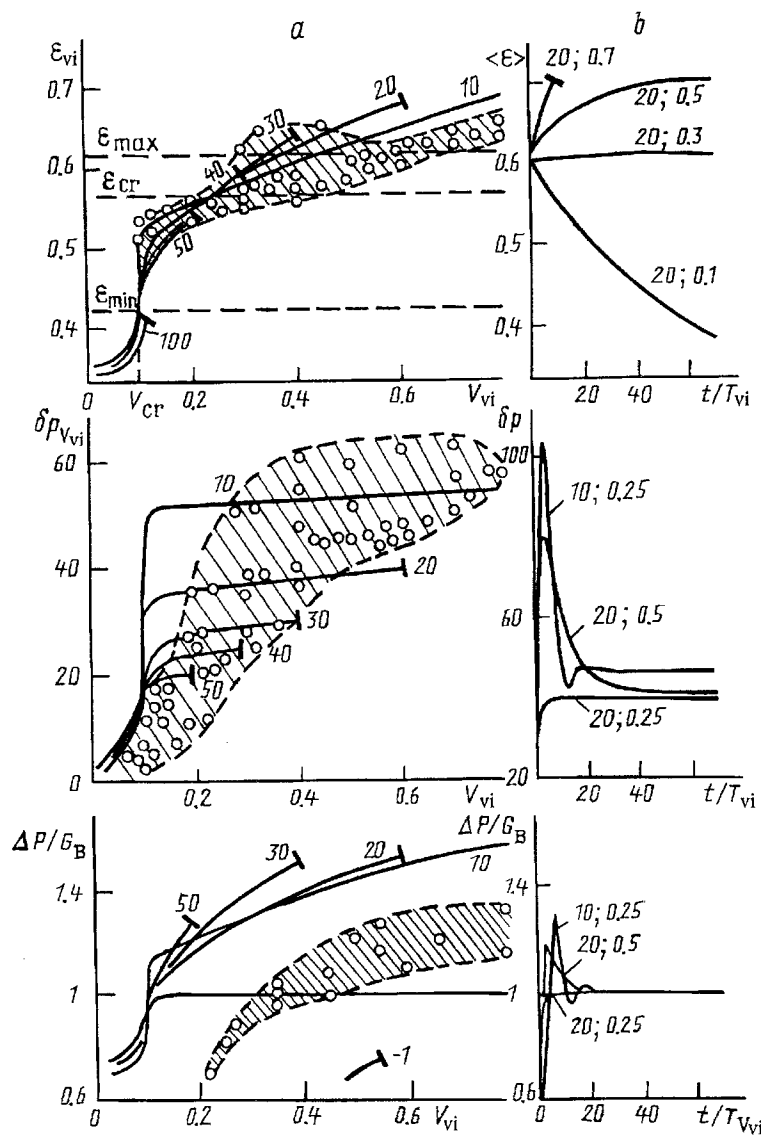


Fig. 2. Parameters of the corundum 70 μm diameter particle vibrobed in the steady state (a) and in the transient process (b): a) figures at the curve, values of f , Hz; experimental data [16]; 1) attainment of the critical frequency Θ_{cr} and end of computation b) figures at the curves, values of f , Hz, and of V_{vi} , m/sec; resonant regime. δp_{vi} , kPa.

Gas Pressure Pulsations. The process of setting up δp repeats the main structural changes of the bed. If the packed bed porosity under vibration does not change, then pressure pulsations achieve their final value "at once." In the expanding layer, due to additional inertia forces an "excess" pulsation peak develops, gradually relaxing to the stationary level. The porosity beats generate a similar process in the pressure.

Energy Consumptions for Vibrofluidization. The active power supplied from the vibroexciter to the model system

$$N_a = 1/(2\pi) \int_{2\pi} \rho \dot{X}_{vi} d\Theta \equiv N_1 + N_2 + \dot{N}_3, \quad (10)$$

is spent in work of the transient expansion process N_1 , in maintaining the stationary suspended state N_2 , and in its hysteresis losses N_3 (Fig. 4). In beds of particles fluidized at $\Theta_V < \Theta_{cr}$, energy consumptions $\sim N_1$ of the transient process dominate over the remaining ones. This must be allowed for when selecting the equipment for vibrofluidization of finely disperse materials that proceeds in the form of a continuous transient process (beats). N_1 is followed by the hysteresis component N_3 of the steady process. Its share in the VB with $\Theta_V < \Theta_{cr}$ is

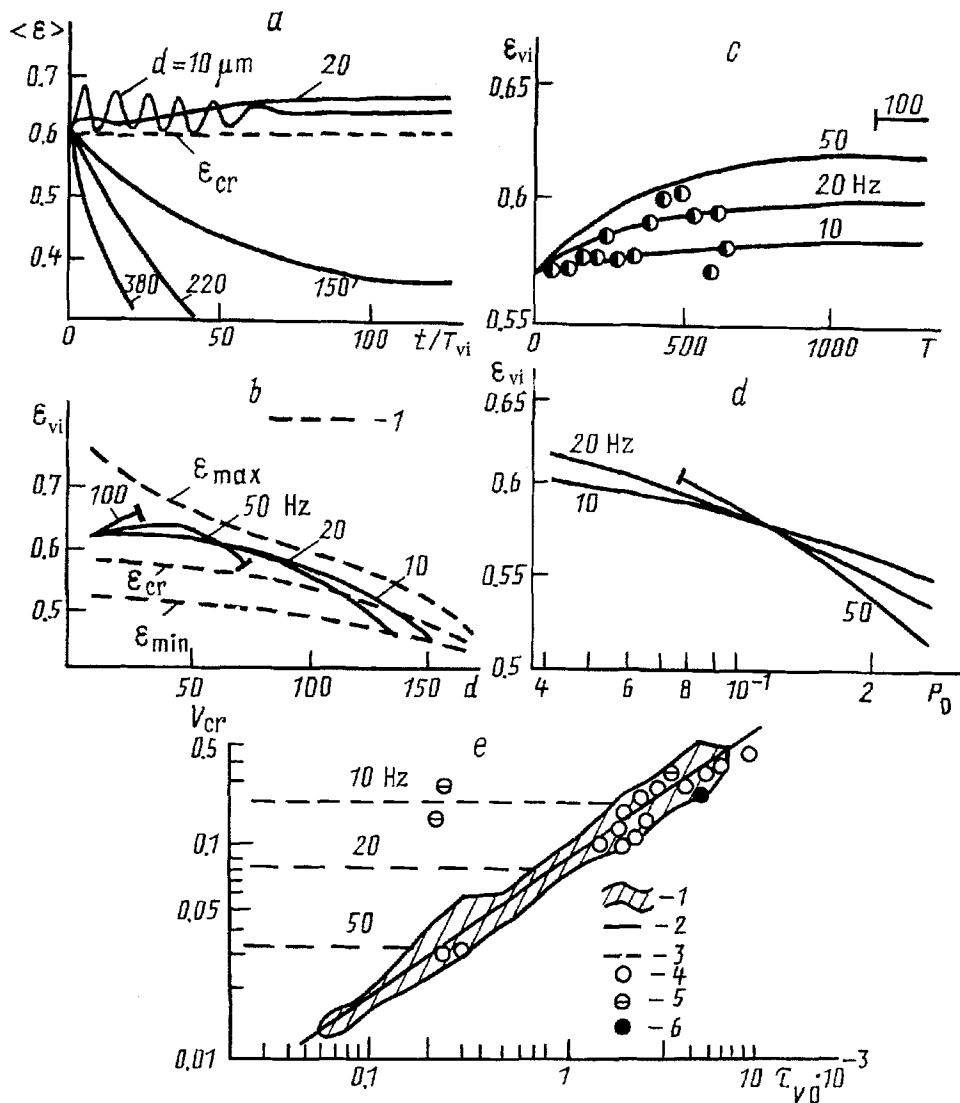


Fig. 3. Dynamics (a) and limiting expansion of the VB vs particle diameter, μm (b), temperature, $^{\circ}\text{C}$ (c), and pressure, MPa (d) according to (1)-(6): a) $V_{vi} = 0.25\text{-}0.5 \text{ m/sec}$, $f = 20 \text{ Hz}$; b) $V_{vi} = 0.25 \text{ m/sec}$, 1) experimental data [5]; c, d) $V_{vi} = 0.25 \text{ m/sec}$, $d = 70 \mu\text{m}$, experimental data [17]; e) critical vibrofluidization velocity; 1) calculated data domain at $p_m = (1\text{-}8) \cdot 10^3 \text{ kg/m}^3$, $P_0 = 0.02\text{-}0.4 \text{ MPa}$, $T = 0\text{-}1600^{\circ}\text{C}$, $d = 40\text{-}100 \mu\text{m}$; 2) course of correlating relation (7); 3) levels of the vibrovelocity V_{α} ; 4) data [21, 16, 17]; 5) [18]; 6) [19]; resonant regime. τ_{v0} , sec.

incommensurably large, as compared to $N_2 \approx N_{FB}$. This defines the high-energy stress and the corresponding process efficiency of the vibrational fluidization method versus the gas one (FB).

4. Vibrofluidization in the Steady State. The limiting state concluding the transient process does not always conform to the true structure of the real vibrobed (see Fig. 2). The best agreement between theory and experiment is achieved for vibration velocities that provide quiescent practically uniform expansion and vibrofluidization of a bed ($V_{vi} = 0.3\text{-}0.4 \text{ m/sec}$ for finely disperse materials) when the system dry friction can be neglected. The quasi-stationary nature of the course of forced oscillations makes it possible here to operate with "rapid" motion components with respect to the very large time interval-averaged ($t \gg T_{vi}$) parameters, to ignore the evolution transitions, and to get rid of the model nonlinearity. The mean porosity, $\epsilon_{vi} \approx \epsilon_0$, of the vibrating bed will be the most important parameter of such an idealized model. From the standpoint of the true process development, this quantity is fictitious since during each period of oscillations the mean porosity $\langle \epsilon \rangle$ may noticeably differ from it.

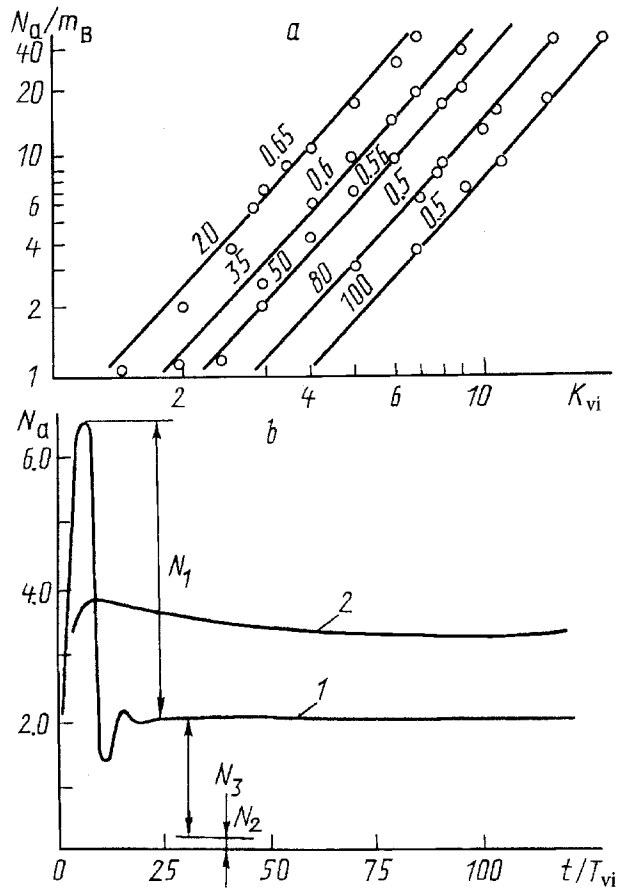


Fig. 4. Energy consumption (kW/m^2) for vibrofluidization of corundum 60-70 μm diameter particles in the steady state and in the transient process; a) calculation by (10): 1) $f=10$ Hz, $V_{vi}=0.25$ m/sec; 2) $f=20$ Hz, $V_{vi}=0.275$ m/sec, $N_2 = G_B v_{cr}$ where v_{cr} is the critical fluidization velocity within the resonant regime.

However, this does not influence the accuracy of the averaged result just perceived by controlling the facilities. Under the mentioned assumptions, the forced oscillations of finely disperse particles in the VB are described by the linear relations obtained from (1)-(6) when the following limits are imposed: $p \ll P_0$, $\dot{m} = \varepsilon = 0$, $\langle \varepsilon \rangle = \varepsilon_{vi} = \varepsilon_0$, $\omega_\varepsilon = \omega_0$, $\tau_V = \tau_{V0}$, $K_{vi} \gg 1$. Their solutions and comparison with pressure pulsation experiment are cited elsewhere in [6]. The hysteresis component of the active energy not calculated previously is determined from the expression

$$N_3 = N_{vi} \eta_N, \quad \eta_N = \Omega^3 \Theta_V / ((1 - \Omega^2)^2 + \Theta_V^2). \quad (11)$$

For small velocities where the bed structure is more dense, failure to account for dry friction results in overestimating the predicted values of the parameters dependent on the bed porosity fluctuation amplitude (δp , ΔP) but does not influence the values of the mean porosity ε_{vi} , for the establishment of which it is sufficient to decrease the dry friction forces of the system for short time.

For larger velocities ($V_{vi} > 0.4$ m/sec) the reverse situation is observed: the experimental data on δp and ΔP lie above the design curves (and the points for ε_{vi} , below). The reasons for such deviations become clear if the process of incipient nonuniform (spouting) vibrofluidization can be presented in the form of a combination of bed expansion and sedimentation sections (see Fig. 1c). It should be noted that since, in the calculation, of the sedimentation process is assumed to proceed slowly, then a transition from the descending curve branches to the ascending ones in Fig. 1c takes place with a jumpwise decrease of $\langle \varepsilon \rangle$. However, already in such a simple simulation, the predicted values both qualitatively and quantitatively instantially approach the experimental ones.

This allows simple engineering methods of calculating dynamic processes within the steady vibrofluidization regime to be developed.

NOTATIONS

a, amplitude; d, particle diameter; f, frequency; g, gravitational acceleration; H, bed height; K_{vi} , relative vibration acceleration; k_ϵ , gas permeability coefficient; m, specific mass (bed gas); N, power; P, p, pressure (gas); T, temperature period; t, time, X, mean-volume structural deformation of a bed; α , reduced internal friction coefficient in a dispersed phase; ϵ , porosity; η , gain factor; Θ , dimensionless vibration frequency; μ , dynamic and kinematic viscosity of the gas; ρ , density (gas); τ_V , phase velocity relaxation time; ω , angular vibration frequency; ω_0 , natural frequency of the suspended bed. Subscripts: vi, vibration; FB, fluidized bed; cr, critical; 0, equilibrium, initial; tr, transient; B, bed; m, particle material; ϵ , current. Symbols, complexes: $a_0 = P_0/(\rho_{B0}\epsilon_0)$; $G_B = m_{BG}$; $K_{vi} = A_{vi}\omega^2/g$; $K_\epsilon = \rho P_0/(\beta H)$; $m_B = \rho_{B0}H_0$; $N_{vi} = 0.5 P_{vi}V_{vi}$; $P_{vi} = \rho_{B0}V_{vi}a_0$; $V_{vi} = A_{vi}\omega$; $X_{vi} = A_{vi} \cos \omega t$; $X = 2/\pi(\epsilon_0 H - \epsilon H)$; $\langle X \rangle_i = 1/T_{vi} \int_0^{T_{vi}} X_i(t) dt$; $\beta(\epsilon) = 150(1-\epsilon)^2 \mu(\epsilon^3 d^2)$; $\Theta = \omega t$; $\Theta_V = \omega T_V$; $\tau_V = \rho_B/\beta = \tau_{V0} \frac{1-\epsilon_0}{1-\epsilon} (\frac{\epsilon}{\epsilon_0})^3$;
 $\Omega = \omega/\omega_0$; $\omega_0 = (\pi/2)(a_0/H)$; $\omega_\epsilon^2 = \omega_0^2 \frac{\epsilon}{\epsilon_0} \frac{1-\epsilon}{1-\epsilon_0}$.

REFERENCES

1. Heat and Mass Transfer Processes in a Fluidized Bed [in Russian], A. P. Baskakov, B. V. Berg, A. F. Ryzhkov, et al. eds., Moscow (1978).
2. A. F. Ryzhkov and V. A. Mikula, *Inzh.-Fiz. Zh.*, **61**, No. 5, 782-789 (1991).
3. Vibrations in Engineering, Handbook in 6 volumes; Volumes 1 and 2, Oscillations of Nonlinear Mechanical Systems [in Russian], I. I. Blekhman, ed., Moscow (1979).
4. V. A. Krasil'nikov and V. V. Krylov, An Introduction to Physical Acoustics [in Russian], Moscow (1984).
5. A. F. Ryzhkov, B. A. Putrik, and V. A. Mikula, *Inzh.-Fiz. Zh.*, **52**, No. 6, 965-974 (1987).
6. A. F. Ryzhkov and B. A. Putrik, *Inzh.-Fiz. Zh.*, **54**, No. 2, 188-197 (1988).
7. R. G. Gutman and J. F. Davidson, *Chem. Eng. Sci.*, **30**, 89-95 (1975).
8. E. F. Karpov, A. S. Kolpakov, B. L. Putrik, et al., *Physicochemical Hydrodynamics* [in Russian], Sverdlovsk (1985), pp. 97-106.
9. V. A. Chlenov and N. V. Mikhailov, *Fluidized Bed* [in Russian], Moscow (1972).
10. I. F. Goncharevich and K. V. Frolov, *Theory of Vibration Engineering and Technology* [in Russian], Moscow (1981).
11. A. F. Ryzhkov, *Flow and Heat/Mass Transfer in Vibrofluidized Disperse Systems*, Doctor's Thesis (Mechanical Engineering), Sverdlovsk (1990).
12. G. S. Mulyava, M. G. Zaitsev, T. N. Bobkova, et al., *Studies of Metallurgy of Antimony, Mercury and Other Metals*, *Tr. Sredaznioprosvetmet.*, No. 18, Tashkent (1977), pp. 20-29.
13. R. Gupta and M. S. Mujumar, *Can. J. Chem. Eng.*, **58**, No. 3, 332-338 (1980).
14. V. A. Borodulya, V. A. Zav'jalov, and J. A. Bujevich, *Chem. Eng. Sci.*, **40**, No. 3, 355-364 (1985).
15. S. S. Zabrodskii, *Flow and Heat Transfer in a Fluidized Bed* [in Russian], Moscow-Leningrad (1963).
16. A. S. Kolpakov, *Heat and Mass Transfer Enhancement in a Finely Disperse Particle Bed due to Vibrofluidization within Resonant Regimes*, Candidates Thesis, Sverdlovsk (1987), pp. 99-106.
17. A. F. Ryzhkov, B. A. Putrik, A. V. Mukovozov, et al., in *Thermal Physics of Nuclear Power Plants*, Sverdlovsk (1987), pp. 99-106.
18. I. L. Zamnius, *Heat and Mass Transfer in Dispersed Devices* [in Russian], Minsk (1970), pp. 60-64.
19. T. Yoshida and Y. Kousaka, *Chem. Eng. Jpn.*, **5**, No. 1, 159-163.
20. A. K. Barakyan, *Heat Transfer Enhancement and Energy Dissipation in Vibrofluidized Bed Equipment*, Thesis, Sverdlovsk (1986).